



**HAL**  
open science

## **Release and toxicity of adipose tissue-stored TCDD: Direct evidence from a xenografted fat model**

Nolwenn Joffin, Philippe Noirez, Jean-Philippe Antignac, Min-Ji Kim,  
Philippe Marchand, Marion Falabrègue, Bruno Le Bizec, Claude Forest,  
Claude Emond, Robert Barouki, et al.

### ► **To cite this version:**

Nolwenn Joffin, Philippe Noirez, Jean-Philippe Antignac, Min-Ji Kim, Philippe Marchand, et al..  
Release and toxicity of adipose tissue-stored TCDD: Direct evidence from a xenografted fat model.  
Environment International, 2018, 121, pp.1113-1120. 10.1016/j.envint.2018.10.027 . hal-01922515

**HAL Id: hal-01922515**

**<https://hal.science/hal-01922515v1>**

Submitted on 14 Nov 2018

**HAL** is a multi-disciplinary open access archive for the deposit and dissemination of scientific research documents, whether they are published or not. The documents may come from teaching and research institutions in France or abroad, or from public or private research centers.

L'archive ouverte pluridisciplinaire **HAL**, est destinée au dépôt et à la diffusion de documents scientifiques de niveau recherche, publiés ou non, émanant des établissements d'enseignement et de recherche français ou étrangers, des laboratoires publics ou privés.

1  
2  
3 **1. Title page**  
4

5 **2 Manuscript title: Release and toxicity of adipose tissue-stored TCDD: direct evidence from a**  
6 **3 xenografted fat model**  
7  
8

9  
10  
11 **5 Names of the authors:** Nolwenn Joffin<sup>1,2\*</sup>, Philippe Noirez<sup>1,2,3,4,5\*</sup>, Jean-Philippe Antignac<sup>6</sup>, Min-ji  
12 Kim<sup>1,6</sup>, Philippe Marchand<sup>7</sup>, Marion Falabregue<sup>2,3,4</sup>, Bruno Le Bizec<sup>7</sup>, Claude Forest<sup>1,2</sup>, Claude  
13 Emond<sup>5,8,9</sup>, Robert Barouki<sup>1,2</sup>, Xavier Coumoul<sup>1,2</sup>  
14  
15

16 **8 Equal contributions (\*) :** Philippe Noirez and Nolwenn Joffin  
17

18  
19 **9 Affiliations of all authors** (department, institution, city, state/province, and country)  
20

21 <sup>1</sup> INSERM UMR-S1124, Toxicologie Pharmacologie et Signalisation cellulaire

22 <sup>2</sup> Université Paris Descartes, 45 rue des Saints-Pères, 75006 Paris, Sorbonne Paris Cité, Paris,  
23 France  
24

25 <sup>3</sup> IRMES, EA 7329, Institut de Recherche bioMédicale et d'Epidémiologie du Sport, Paris, France

26 <sup>4</sup> Institut National du Sport, de l'Expertise et de la Performance (INSEP), Paris, France

27 <sup>5</sup> Université du Québec à Montréal (UQAM), Montreal, Qc, Canada

28 <sup>6</sup> Université Paris 13, Sorbonne Paris Cité, Bobigny, France

29 <sup>7</sup> Laboratoire d'Etude des Résidus et Contaminants dans les Aliments (LABERCA), UMR 1329 Oniris-  
30 INRA, Nantes, France  
31

32 <sup>8</sup> BioSimulation Consulting Inc, Newark, DE, USA, 19713

33 <sup>9</sup> Université de Montréal, Montreal, Qc, Canada  
34  
35

36  
37  
38  
39 **22 Name of and contact information for corresponding authors:** X. Coumoul<sup>1,2</sup>; phone:  
40 +33142863359; fax: +33142863868; email: [xavier.coumoul@parisdescartes.fr](mailto:xavier.coumoul@parisdescartes.fr); R. Barouki<sup>1,2</sup>;  
41 phone: +33142862075; fax: +33142863868; email: [robert.barouki@parisdescartes.fr](mailto:robert.barouki@parisdescartes.fr)  
42  
43

44 **25 Running title:** PBPK model describing POPs release by fat tissue  
45  
46

47  
48  
49 **27 Acknowledgments and funding:** This work was supported by the ANSES (ALLOFATOX-Funding  
50 including PhD fellowship: N. Joffin), the Université Paris Descartes-COMUE-SPC (Funding), INSERM  
51 (Funding), Assistance Publique-Hôpitaux-de-Paris, the LUNAM Université (Funding).  
52

53  
54 **30 A competing financial interest's declaration:** all authors have disclosed that there is no actual or  
55 potential competing interest regarding the submitted article  
56  
57  
58  
59

60  
61  
62  
63  
64  
65  
66  
67  
68  
69  
70  
71  
72  
73  
74  
75  
76  
77  
78  
79  
80  
81  
82  
83  
84  
85  
86  
87  
88  
89  
90  
91  
92  
93  
94  
95  
96  
97  
98  
99  
100  
101  
102  
103  
104  
105  
106  
107  
108  
109  
110  
111  
112  
113  
114  
115  
116  
117  
118

32  
  
33  
34  
35  
36  
37  
38  
39  
40  
41  
42  
43  
44  
  
45  
  
46  
  
47  
48  
49  
50  
  
51  
  
52

**List of abbreviations:** alpha-SMA: alpha-smooth muscle actin; AhR: aryl hydrocarbon receptor; AQP: aquaporin; AT: adipose tissue; ATGL: adipose triglyceride lipase; bw: body weight; CD: cluster of differentiation; COL1A1: collagen 1A1; CPT1B: carnitine palmitoyl-transferase 1B; CYP: cytochrome P450; FABP4: fatty acid binding protein 4; FAS: fatty acid synthase; G6Pase: glucose-6 phosphatase; HSL: hormone-sensitive lipase; IL: interleukin; MCP-1: monocyte chemoattractant protein-1; NOS2: NO Synthase 2; PAI-1: plasminogen activator inhibitor-1; PBPK: Physiologically based pharmacokinetic; PC: pyruvate carboxylase; PCB: polychlorinated biphenyl; PDK: pyruvate dehydrogenase kinase; PECK: phosphoenolpyruvate carboxykinase; PGC-1 alpha: PPARγ-coactivator 1 alpha; POPs: Persistent Organic Pollutants; PPARα: peroxisome proliferator-activated receptor-alpha; PPARγ2: PPAR-gamma2; RT-qPCR: real-time quantitative PCR; SD: Standard Deviation; TNF: Tumor-Necrosis Factor; UCP1: uncoupling protein 1; VLCAD: Very long-chain acyl-CoA dehydrogenase; PBPK: Physiologically Based Pharmacokinetic.

### Highlights

- A new model to study the release and distribution of POPs
- Introduction of a new PBPK model to study the effects of POPs
- Internal release of TCDD activates signatures of inflammation & fibrosis.
- Internal stores of POPs could play a significant role in long term toxicity.

119  
120  
121  
122  
123  
124  
125  
126  
127  
128  
129  
130  
131  
132  
133  
134  
135  
136  
137  
138  
139  
140  
141  
142  
143  
144  
145  
146  
147  
148  
149  
150  
151  
152  
153  
154  
155  
156  
157  
158  
159  
160  
161  
162  
163  
164  
165  
166  
167  
168  
169  
170  
171  
172  
173  
174  
175  
176  
177

53 **2. Abstract.**

54 **Background:** Persistent organic pollutants (POPs) are known to accumulate in adipose tissues (AT).  
55 This storage may be beneficial by diverting POPs from other sensitive tissues or detrimental because  
56 of chronic release of pollutants as indirectly suggested during weight loss. The aim is to study the  
57 biological and/or toxic effects that chronic POP release from previously contaminated grafted AT could  
58 exert in a naïve mouse. **Methods:** C57BL/6J male mice were exposed intraperitoneally to 2,3,7,8-  
59 tetrachlorodibenzo-p-dioxin (TCDD); their epididymal fat pads were collected and grafted on the back  
60 skin of uncontaminated recipient mice whose brain, liver, and epididymal ATs were analyzed (TCDD  
61 concentration, relevant gene expression). Kinetics of release and redistribution were modeled using  
62 Physiologically Based Pharmacokinetics (PBPK). **Results:** The grafts released TCDD over a period of 10  
63 weeks with different kinetics of distribution in the three organs studied. A PBPK model was used to  
64 simulate the AT releasing process and the incorporation of TCDD into the major organs. At three weeks  
65 post-graft, we observed significant changes in gene expression in the liver and the host AT with  
66 signatures reminiscent of inflammation, gluconeogenesis and fibrosis as compared to the control.  
67 **Conclusions:** This study confirms that AT-stored TCDD can be released and distributed to the organs  
68 of the recipient hence leading to distinct changes in gene expression. This original model provides  
69 direct evidence of the potential toxic-relevant effects when endogenous sources of contamination are  
70 present.

71

72 **Keywords:** adipose tissue, graft, internal release, dioxin, TCDD, PBPK, fibrosis

73

178  
179  
180 **74 3. Introduction**  
181

182 75 Persistent organic pollutants (POPs) are xenobiotics of major concern for environmental health  
183 76 (Bonde et al., 2016; Mostafalou, 2016; Smarr et al., 2016). 2,3,7,8-tetrachlorodibenzo-p-dioxin (TCDD)  
184 77 is one of the most potent compounds among the dioxin class of substances and its toxicity equivalence  
185 78 factor is set to a reference value of 1. TCDD binds to the Aryl hydrocarbon Receptor (AhR), a protein of  
186 79 the basic Helix-Loop-Helix / Per - ARNT - Sim (bHLH/PAS) family, which transcriptionally activates the  
187 80 expression of genes which code for xenobiotic metabolizing enzymes (XME) as well as that of other  
188 81 genes (Guyot *et al.* 2013). However, in spite of the induction of these detoxifying enzymes, the TCDD  
189 82 and other POPs are very poorly metabolized and, therefore, not readily eliminated. This, as well as  
190 83 their lipophilicity, accounts for their accumulation in adipose tissue (AT) (Lee *et al.* 2017).  
191

192 84 The storage of POPs in AT is believed to have complex implications and consequences (Kim *et*  
193 85 *al.* 2011, 2012). It may be protective to a certain extent since it diverts POPs from critical target organs  
194 86 such as the brain. However, it is also assumed that contaminated AT progressively delivers POPs that  
195 87 would eventually lead to a chronic low-rating release resulting in chronic toxicity. Indeed, we and  
196 88 others observed an increase in blood POPs following weight loss (Chevrier *et al.* 2000, Imbeault *et al.*  
197 89 2002, Kim *et al.* 2011) but such increase could also be the result of the dynamic switch between  
198 90 lipolysis and lipogenesis that occurs during fasting/feeding process, independent of weight loss. The  
199 91 evidence for both scenarios, *i.e.* protection and long-term toxicity, is indirect at this stage.  
200

201 92 Long-term exposure to TCDD has been associated with many pathologies including cancer,  
202 93 infertility or metabolic diseases (White and Birnbaum, 2009). Its carcinogenic effects have been  
203 94 established by the World Health Organization (WHO) and the US National Toxicology Program (NTP)  
204 95 despite some conflicting results in humans (Boffetta *et al.* 2011). Regarding metabolic diseases, a  
205 96 recent meta-analysis pointed to a likely link between TCDD exposure and type 2 diabetes (Goodman  
206 97 *et al.* 2015), while *in vitro* and *in vivo* experiments showed that TCDD reduced glucose uptake by the  
207 98 liver and AT, a process that occurs with decreases in insulin production and secretion by beta-  
208 99 pancreatic cells (Novelli *et al.* 2005). TCDD is also suspected to elicit metabolic diseases through either  
209 100 the induction of local inflammation of the AT (Kim *et al.* 2012), the regulation of endogenous  
210 101 metabolizing enzymes (carbohydrate and lipid pathways) (Ambolet-Camoit *et al.* 2015) or epigenetic  
211 102 mechanisms. Such TCDD effects are consistent with the suspected obesogen effects of several POPs  
212 103 (*i.e.* organochlorinated pesticides) (La Merrill *et al.* 2013; Lee *et al.* 2014).  
213  
214  
215  
216  
217  
218  
219  
220  
221  
222  
223  
224  
225  
226  
227  
228

229 104 While the long-term toxicity of TCDD (and other POPs) is now established, there is still no direct  
230 105 evidence that its release from AT is involved in such long-term toxicity although such effects are being  
231 106 suspected (Kim *et al.* 2011). In all experimental protocols, animals are either fed or injected with TCDD,  
232  
233  
234  
235  
236

237  
238  
239  
240  
241  
242  
243  
244  
245  
246  
247  
248  
249  
250  
251  
252  
253  
254  
255  
256  
257  
258  
259  
260  
261  
262  
263  
264  
265  
266  
267  
268  
269  
270  
271  
272  
273  
274  
275  
276  
277  
278  
279  
280  
281  
282  
283  
284  
285  
286  
287  
288  
289  
290  
291  
292  
293  
294  
295

107 resulting in single (or repetitive) exposures. There are several possible mechanisms for long-term  
108 toxicity. Such toxicity may be due to the direct effect of ingested TCDD following exposure but could  
109 also be additionally due to TCDD output from internal compartments like AT. Because of the lack of an  
110 experimental model assessing the role of AT-stored TCDD, it has not been possible yet to assess those  
111 hypotheses and to clearly identify the kinetic and dynamic behaviors of TCDD discharged from internal  
112 storage sites.

113 The aims of the present study were 1) to develop an experimental model based on a surgical  
114 graft procedure; 2) to describe the fate and effects of AT-stored TCDD then specifically investigate  
115 whether this compound can be discharged from the AT and display activity on other tissues, and 3) to  
116 build a physiologically based pharmacokinetic (PBPK) model to simulate the distribution of TCDD by  
117 gavage and the donor, and then at the second time simulating a chronic endogenous POP release from  
118 the graft implant in the host, and 4) to characterize the effects of this release on the expression of  
119 several biomarkers linked to pathologies. To achieve this goal, we have developed a unique, new and  
120 original experimental model allowing such investigation. We have grafted TCDD-contaminated AT to  
121 uncontaminated mice and monitored the action that sub-chronic release of this POP could exert in  
122 three host tissues, AT, liver and brain; such novel bioengineered mice allowed the generation of a PBPK  
123 model simulating a chronic POP output from a grafted implant. We characterized the effects of this  
124 release on the expression of several biomarkers linked to the above-described pathologies - including  
125 endogenous metabolic enzymes or inflammatory cytokines - in recipient AT and liver, two organs that  
126 are critically involved in metabolic regulations.

127

296  
297  
298  
299  
300  
301  
302  
303  
304  
305  
306  
307  
308  
309  
310  
311  
312  
313  
314  
315  
316  
317  
318  
319  
320  
321  
322  
323  
324  
325  
326  
327  
328  
329  
330  
331  
332  
333  
334  
335  
336  
337  
338  
339  
340  
341  
342  
343  
344  
345  
346  
347  
348  
349  
350  
351  
352  
353  
354

## 128 4. Materials and Methods

### 129 4.1 Mice

130 The European Communities Council Directive 2010/63/EU on the protection of the animals  
131 was followed for the experiments using animals. All procedures were approved by the ethical  
132 committee for animal research of Paris Descartes university (CEEA.34, number: 12-132). C57BL/6J  
133 male mice (12-week-old) with body weight (bw) about 25 g were obtained from Janvier and allowed 1  
134 week to acclimate at the Paris Descartes university animal facility before the study. Animals were  
135 maintained on a 12-hr light/dark cycle at the ambient temperature of a  $22 \pm 1^\circ\text{C}$  and relative humidity  
136 of  $55 \pm 5\%$  and were provided with Purina 5001 rodent Chow (Safe) and tap water ad libitum.

### 138 4.2 Primary POPs exposure

139 The mice donor C57BL/6J received a single intraperitoneal injection with either dose of 0, 1,  
140 10 or 25  $\mu\text{g}$  TCDD/kg of bw in corn oil. Mice were sacrificed 48h after injection. For each mouse, both  
141 epididymal fat pads were collected: one was used for TCDD quantification and the other for the graft  
142 to a donor mouse.

### 144 4.3 Graft of epididymal AT contaminated with POPs

145 Each epididymal fat pad was grafted into the subcutaneous plane on the back of the mice.  
146 Mice were sacrificed at 0.5, 1, 2, 3, 4 or 10 weeks following the graft. The graft, brain, liver, and  
147 epididymal AT were removed for quantification of TCDD and gene analyses. We observed that the  
148 grafts were revascularized between 4 and 10 weeks following the surgical procedure (data not shown).

### 150 4.4 POPs internal exposure levels quantification

151 The methodology that was applied to isolate, detect, and quantify TCDD had its origin in a  
152 more global previously described method used for measuring dioxins and PCBs (Costera et al. 2006).  
153 Briefly,  $^{13}\text{C}$ -labelled TCDD was added to each sample for quantification according to the isotopic  
154 dilution method. Samples of AT (50 to 250 mg), liver (0.150 to 1.750 g) and brain (150 to 550 mg) were  
155 first submitted to an accelerated solvent extraction at high temperature and high pressure (ASE  
156 Dionex, Sunnyvale, CA). The resulting extracts were weighed to evaluate fat content by a gravimetric  
157 method and were reconstituted in hexane for further sample clean up through three purification steps  
158 using successively acid silica, florisil, and celite/carbon columns. TCDD concentrations were assessed  
159 using gas chromatography (Agilent 7890A) coupled to high-resolution mass spectrometry (GC-HRMS)  
160 on electromagnetic sector instrument (JEOL MS 800D), operating at 10,000 resolutions and in the  
161 single ion monitoring (SIM) acquisition mode. This method was validated according to current

355  
356  
357  
358  
359  
360  
361  
362  
363  
364  
365  
366  
367  
368  
369  
370  
371  
372  
373  
374  
375  
376  
377  
378  
379  
380  
381  
382  
383  
384  
385  
386  
387  
388  
389  
390  
391  
392  
393  
394  
395  
396  
397  
398  
399  
400  
401  
402  
403  
404  
405  
406  
407  
408  
409  
410  
411  
412  
413

162 European criteria in the field of regular control of foodstuff of animal origin and accredited according  
163 to the ISO 17025 standard.

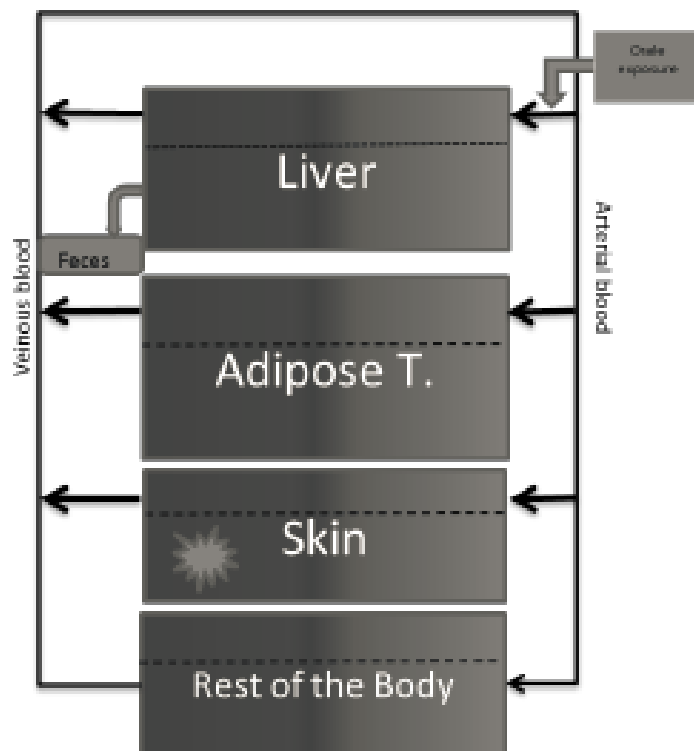
164  
165 **4.5 PBPK modeling**

166 Several models have been published to mimic the pharmacokinetics of TCDD on different  
167 species (Emond, 2004; Kissel and Robarge, 1998; Leung et al., 1990, 1988). More recently, a PBPK  
168 model for TCDD has been applied to humans and mice (Emond et al., 2010; Emond et al., 2016) to  
169 study the influence of obesity and diabetes on the elimination of TCDD (Emond et al., 2018). A larger  
170 description and assessment work of the PBPK model for mice were performed and peer-reviewed  
171 during the NCEA-USEPA reassessment (USEPA, 2012). This version of the PBPK model was used as a  
172 base for the present work. Briefly, the model is originally composed of 3 compartments (liver, AT and  
173 the rest of the body) connected to the systemic circulation (arterial and venous). The rest of the body  
174 compartment is composed of muscles ( $\approx 70\%$ ) and other non-essential organs for the pharmacokinetics  
175 but is required for the mass balance calculation. The rest of the body is then described as permeability-  
176 limited compartments (composed of extracellular matrix and blood sub-compartments). The  
177 elimination of TCDD from the body is very limited; it happens mostly in the feces and not much in the  
178 urine. In addition, the PBPK model also integrates an enterohepatic cycle; overall, it allows the  
179 description of an elimination rate based on the body burden using a mathematical component function  
180 (Emond et al. 2016; USEPA 2012). One key parameter of this model, which conditions the elimination  
181 rate of TCDD, is the induction of CYP1A2 which is due to AhR activation (CY1A2 is a transcriptional  
182 target of the AhR) which depends on the body burden (Diliberto et al. 1997; Emond *et al.* 2005, 2006).  
183 All the parameters used in this PBPK model, before modification, were previously assessed and  
184 presented in the USEPA 2012 report (in this reference, see Tables 3-8 pages 3-63).

185 To describe the release of TCDD from the AT implanted in the dorsal subcutaneous skin region  
186 (graft), it was necessary to update the original PBPK model by adding a skin compartment and graft  
187 (Figure 1).



414  
415  
416  
417  
418  
419  
420  
421  
422  
423  
424  
425  
426  
427  
428  
429  
430  
431  
432  
433  
434  
435  
436  
437  
438  
439  
440  
441  
442  
443  
444  
445  
446  
447  
448  
449  
450  
451  
452  
453  
454  
455  
456  
457  
458  
459  
460  
461  
462  
463  
464  
465  
466  
467  
468  
469  
470  
471  
472



188

**Figure 1:** Conceptual representation of the PBPK model in mice

189

Indeed, we assumed that the graft was an entity added to the skin compartment. Basically, the graft releases the TCDD which diffuses to the skin compartment and is then released in the blood. The blood flow in the skin compartment was described as permeability-limited; all parameters for this additional compartment including the partition coefficient “skin/ blood” (unitless), perfusion of the skin compartment ( $\text{ml}\cdot\text{h}^{-1}$ ), the diffusion permeability of the skin ( $\text{ml}\cdot\text{h}^{-1}$ ) and the volume of skin tissue (ml) were extracted from the literature (Brown *et al.*, 1997; Wang *et al.*, 1997) (Table 1).

196

197

198 **Table 1: physiological parameters used to define both skin and graft compartments used in the PBPK**  
 199 **allografted mice model**

Parameters	Name of the parameters	values	references
$V_{sk}$	Fraction of body weight for skin (unitless)	0.165	Brown <i>et al.</i> , 1997
$V_{skb}$	Fraction of tissue blood volumes for skin (unitless)	0.0159	Wang <i>et al.</i> , 1997
$Q_{skf}$	Tissue blood flow fraction of cardiac output for skin (unitless)	0.057	Brown <i>et al.</i> , 1997
$P_{sk/b}$	Partition coefficient (skin/blood) (unitless)	10	Wang <i>et al.</i> , 1997
KGRAFT	First order parameter of TCDD release in graft to the skin ( $h^{-1}$ )	0.004	Optimized
PASKINF	Diffusion permeability (unitless)	0.09	Optimized
R	Fraction of blood diffusion (PASKIN) from the blood skin to the grafted starting 4 weeks post graft implantation (unitless)	R= 0.0007	Optimized

200  
 201 The graft sub-compartment is essentially composed of TCDD-delivering AT (see §4.2). This  
 202 delivery was estimated using the concentration of TCDD in the graft at time 0 and the subsequent  
 203 measurements at different time points (using a first order kinetic release of TCDD from the graft to the  
 204 skin). We also consider a functional vascularization of the graft around week 4 (visual observation).  
 205 The parameters used to mimic mathematically the release of TCDD from the graft are presented in  
 206 Table 2:

208 **Table 2: Parameters used to mimic mathematically the release of TCDD from the graft in the**  
 209 **corresponding equations**

Parameters	Description of the parameters
cgraft0	concentration of TCDD in the graft at time 0 ( $pg.g^{-1}$ )
graftmass	mass of the graft (g)
agraftpg	amount of TCDD at time 0 (pg)
kgraft	constant transfer of TCDD from graft to skin ( $h^{-1}$ )
agraftng	amount of TCDD in the graft at time 0 (ng)
agraftnmol	amount of TCDD in the graft at time 0 (nmole)
agraftresnmol	amount of TCDD remaining in the graft at different time points (nmole)

532  
533  
534  
535  
536  
537  
538  
539  
540  
541  
542  
543  
544  
545  
546  
547  
548  
549  
550  
551  
552  
553  
554  
555  
556  
557  
558  
559  
560  
561  
562  
563  
564  
565  
566  
567  
568  
569  
570  
571  
572  
573  
574  
575  
576  
577  
578  
579  
580  
581  
582  
583  
584  
585  
586  
587  
588  
589  
590

211 The amount of TCDD which remains in the graft after each time point (dt), also *agraftresnmol*,  
212 was estimated using **equation 1**:

- **Equation 1:** variation of the amount of TCDD (nmole) that remains in the graft after each time interval (dt) in hours

$$\frac{d\text{agraftnmol}(\text{nmol})}{dt(\text{h})} = -k\text{graft} \times \text{agraftresnmol}$$

219 Then, the changes in TCDD concentrations in the grafts were estimated using **equations 2 & 3**.

- **Equation 2** Amount of TCDD (nmoles) remaining in the graft after each time point (dt):

$$\text{agraftresnmol} = \int_{t-1}^t \text{agraftnmol}$$

- **Equation 3:** Concentration of TCDD in pg/g

$$\text{agraftrespgg}\left(\frac{\text{pg}}{\text{g}}\right) = \text{agraftresnmol}(\text{nmole}) \times \frac{MW\left(\frac{\text{ng}}{\text{nmole}}\right) \times 1000\left(\frac{\text{pg}}{\text{ng}}\right)}{\text{graftmass}(\text{g})}$$

228 These simulation parameters were optimized by a first series of experiments carried out to  
229 assess the release of TCDD from the graft during the optimization of the exposure dose of the donor.  
230 Determination of the graft mass and the concentration of TCDD at different time points were  
231 compared to the simulation profile resulting from the model. In addition, simulation of TCDD  
232 generated using the PBPK model was compared to the experimental time points determined  
233 experimentally.

#### 4.6 RNA sampling from tissues

236 AT and liver samples were placed in 1 mL of Qiazol® reagent with 2 stainless steel beads  
237 (Qiagen, France) and were homogenized with a TissueLyser system (RetschMM300, Germany). Total  
238 RNA was prepared using the RNeasy Mini Kit following the manufacturer's instructions (Qiagen,  
239 France). The quality of total RNA was monitored with a Nanodrop ND-1000 spectrophotometer  
240 (Nanodrop products, Wilmington, USA).

591  
592  
593 **248 4.7 Quantitative real-time PCR**  
594

595 **249** Reverse transcription was carried out using the High Capacity cDNA Reverse Transcription Kit  
596 (Life technology, France) according to the manufacturer's directions. Real-time PCR was achieved with  
597 **250**  
598 **251** 20 ng of cDNA, with duplicates for each experiment. STable 1 (Suppl Mat.) gives the gene-specific  
599  
600 **252** primers. The relative amounts of mRNA were estimated using the  $\Delta\Delta C_T$  method with Ribosomal Protein  
601 **253** L13 (RPL13) as the reference gene (Juricek *et al.*, 2014; Pfaffl, 2001).  
602  
603 **254**

Gene	Forward primer	Reverse primer
AhR	ACAGTAAAGCCCATCCCC	AGCACAAAGCCATTTCAGC
CYP1A1	ATGAGTTTGGGGAGGTTACTG	AATGAGGCTGTCTGTGATGTC
CYP1B1	GAGGATGTGCCTGCCACTA	CTGTGGCTGCTCATCCTCTT
IL-1 $\beta$	GCCACCTTTTGACAGTGATG	TCTCCACAGCCACAATGAG
IL-6	CTTCCATCCAGTTGCCTTCTTG	AATTAAGCCTCCGACTTGTGAAG
TNF alpha	TCATCCATTCTCTACCCAGC	GTCCCAGCATCTTGTGTTTC
MCP-1	AGCAGCAGGTGTCCCAAAGA	ACGGGTCAACTTCACATTCAA
NOS2	TGAGGGGACTGGACTTTTAG	CTGTGACTTTGTGCTTCTGC
F4/80	TTTCTCGCCTGCCTCTTC	CCCCGTCTCTGTATTCAACC
COL1A1	TCATCGTGGCTTCTCTG	CGTTGAGTCCGTCTTTG
Alpha-SMA	CCTGGTGTGCGACAATG	TGCTCTGGGCTTCATCC
Glycogen synthase 2	CCAGCTTGACAAGTTCGACA	ATCAGGCTTCTCTTCAGCA
PC	CGGCAGGGCGGAGCTAACAT	TTTGGGGAGGCAACAGGGGC
PEPCK-c	AGTGCCCCATTATTGACC	TCTTGCCCTTGTGTTCTG
G6Pase	CCAAGGGAGGAAGGATG	AGGTGACAGGGAAGTCT
PGC-1 alpha	TGCCCTGCCAGTCACAGGA	GCTCAGCCGAGGACACGAGG
RPL13	GGATCCCTCCACCCTATGACA	CTGGTACTTCCACCCGACCTC
CD68	CCAATTCAGGGTGAAGAAA	CTCGGGCTCTGATGTAGGTC
AQP7	GAAGTCAAGGCTTGGTCTGCT	CATGTGAGCCACGGAACCAA
ATGL	CCAACGCCACTCACATC	CAGAGGACCCAGGAACC
HSL	ACTGAGATTGAGGTGCTGTC	AAGGCAGGTGAGATGGTAAC
CPT1B	TTCCGACAAACCCTGAAGCT	TAAGATCTGGGCTATCTGTGTC
VLCAD	TGAATGACCCTGCCAAG	CCACAATCTCTGCCAAGC
CD36	CATGAGAATGCCTCCAAACAC	GGAAGTGTGGGCTCATTGC
GLYCOGEN KINASE	ATCCGCTGGCTAAGAGACAACC	TGCACTGGGCTCCCAATAAGG
PDK4	TGTGATGTGGTAGCAGTAGTC	ATGTGGTGAAGGTGTGAAG
FABP4	AACACCGAGATTTCTT	ACACATTCCACCACCAG
PPAR $\alpha$	AAGCCATCTTCACGATGCTG	TCAGAGGTCCCTGAACAGTG
FAS	TCCTGGGAGGAATGTAAACAGC	CACAAATTCATTACTGCAGCC
UCP1	CCGCGACTTCGGACTCCTGC	TAACGGGTCTCCTGCCCG
PPAR $\gamma$ 2	TTATGCTGTTATGGGTGAAA	CAAAGGAATGCGAGTGGTC

644 **255**  
645 **256** **Supplementary table S1: list of primers used for quantitative RT-PCR experiments**  
646  
647  
648  
649

650  
651  
652  
653  
654  
655  
656  
657  
658  
659  
660  
661  
662  
663  
664  
665  
666  
667  
668  
669  
670  
671  
672  
673  
674  
675  
676  
677  
678  
679  
680  
681  
682  
683  
684  
685  
686  
687  
688  
689  
690  
691  
692  
693  
694  
695  
696  
697  
698  
699  
700  
701  
702  
703  
704  
705  
706  
707  
708

257  
258  
259  
260  
261  
262  
263

**4.8 Statistical analyses**

Unless otherwise specified, two-group and multiple-group comparisons were made using Mann-Whitney's U-test (nonparametric comparison of two independent series) or Kruskal-Wallis test followed by a pair-wise Dunn's post hoc test (nonparametric comparison of multiple independent series). A p-value < 0.05 was considered statistically significant (\*\* p<0.01, \* p<0.05). The values are expressed as the mean ± standard deviation.

709  
710  
711 264 **5. Results**

712  
713 265 **5.1 Xenografted-adipose tissue releases TCDD**

714  
715 266 Vehicle (control) or three different doses of TCDD (1, 10 or 25  $\mu\text{g}\cdot\text{kg}^{-1}$  bw; corn oil as a control)  
716 267 were intraperitoneally injected to C57BL6/J male mice that were sacrificed 48h later. TCDD  
717 268 concentration was determined in the epididymal AT of control (corn oil) and exposed mice, showing a  
718 269 proportional increase in the TCDD levels in line with the injected doses (STable 2, Suppl. Mat.).

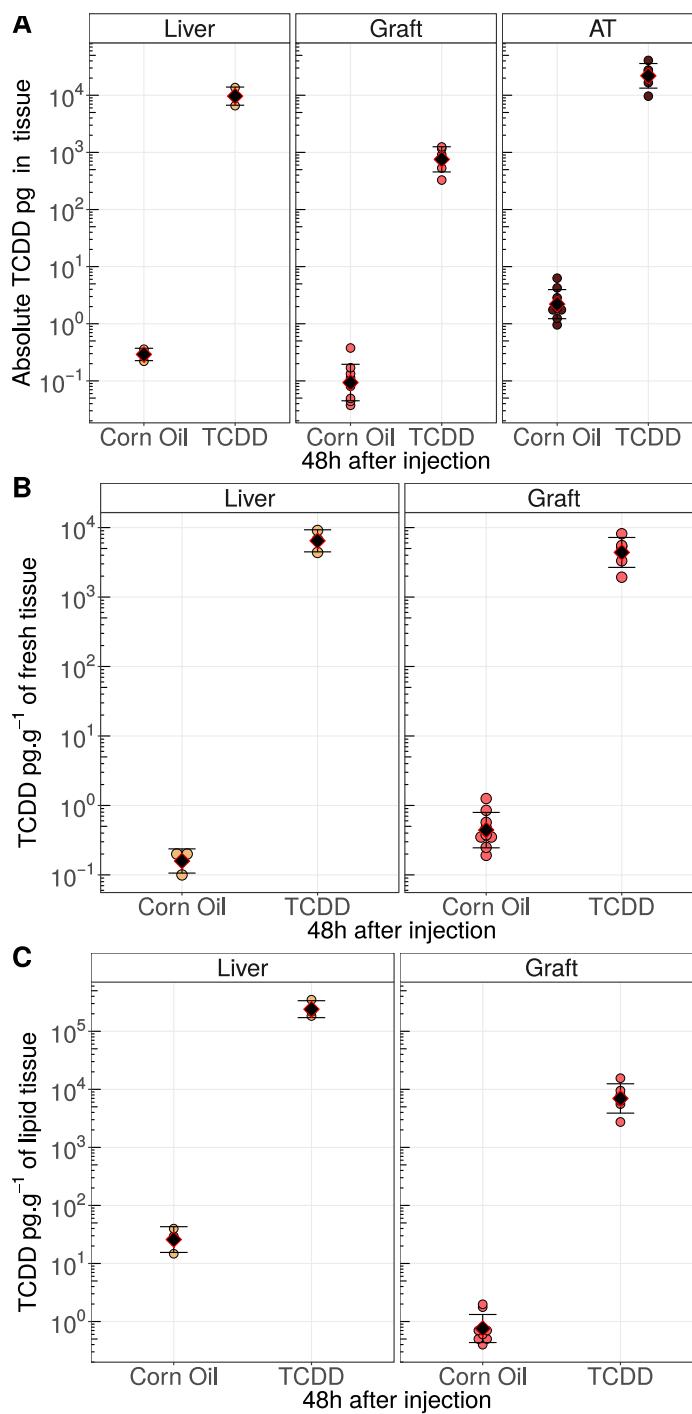
722  
723  
724  
725  
726  
727  
728  
729  
730  
731  
732

TCDD dose ( $\mu\text{g}\cdot\text{kg}^{-1}$ bw)	Levels of TCDD in the AT 48h later ( $\text{pg}\cdot\text{g}^{-1}$ fresh tissue)	Relative fold increase in the AT
0	6	-
1	2 335	1
10	21 623	9
25	56 608	24

733 270  
734 271 **Supplementary table S2: comparison of TCDD-injected doses ( $\mu\text{g}\cdot\text{kg}^{-1}$  bw) in C57BL/6J male**  
735  
736 272 **mice and its levels in the AT ( $\text{pg}\cdot\text{g}^{-1}$  fresh tissue) 48h after injection.**

737 273  
738  
739  
740 274 The dose of 10  $\mu\text{g}\cdot\text{kg}^{-1}$  bw did not saturate the AT since higher concentrations of TCDD in the  
741 275 AT were obtained following the injection of 25  $\mu\text{g}\cdot\text{kg}^{-1}$  TCDD; thus, this dose (10  $\mu\text{g}\cdot\text{kg}^{-1}$  bw) was  
742  
743 276 selected for all subsequent experiments (SFigure 1, Suppl Mat.).  
744  
745  
746  
747  
748  
749  
750  
751  
752  
753  
754  
755  
756  
757  
758  
759  
760  
761  
762  
763  
764  
765  
766  
767

768  
769  
770  
771  
772  
773  
774  
775  
776  
777  
778  
779  
780  
781  
782  
783  
784  
785  
786  
787  
788  
789  
790  
791  
792  
793  
794  
795  
796  
797  
798  
799  
800  
801  
802  
803  
804  
805  
806  
807  
808  
809  
810  
811  
812  
813  
814  
815  
816  
817  
818  
819  
820  
821  
822  
823  
824  
825  
826

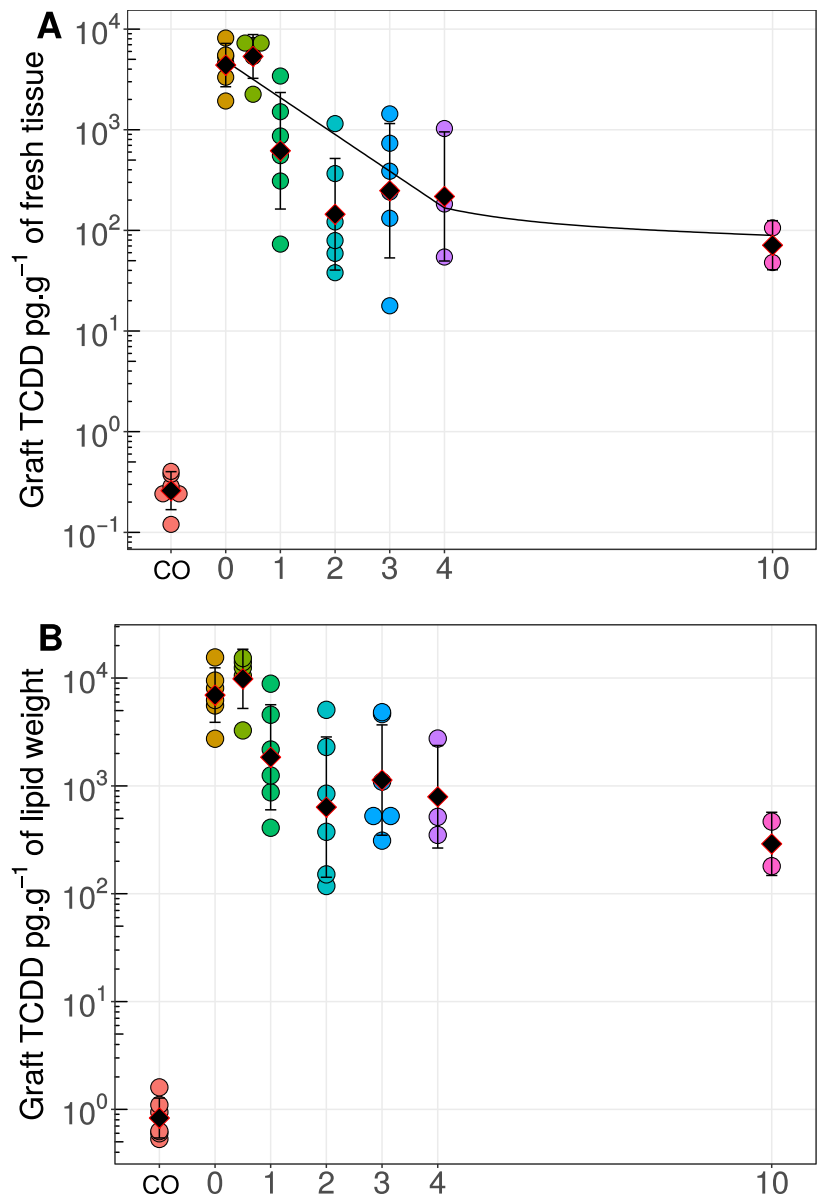


277

278 **Figure 1:** Global burden (pg, A) and concentration levels (pg.g<sup>-1</sup> fresh tissue, B and pg.g<sup>-1</sup> lipid tissue,  
279 C) of TCDD determined in the liver, the graft, and/or the whole AT of the mice donors which had  
280 received a single intraperitoneal injection (see §4.2). The levels of TCDD were measured in the liver  
281 and the AT; the upper panel represents the absolute quantity (in pg) of TCDD in the liver, the  
282 epididymal AT (used later as a graft) and the extrapolated whole-body AT; the middle and lower panels  
283 represent the concentration of TCDD (respectively in pg.g<sup>-1</sup> of fresh tissue or pg.g<sup>-1</sup> of lipids). One of  
284 the epididymal AT (the left one) has been used as a graft (weight of the graft: 100-150 mg;  
285 approximated concentration of TCDD: 10<sup>4</sup> pg.g<sup>-1</sup> of lipids).

827  
828  
829  
830  
831  
832  
833  
834  
835  
836  
837  
838  
839  
840  
841  
842  
843  
844  
845  
846  
847  
848  
849  
850  
851  
852  
853  
854  
855  
856  
857  
858  
859  
860  
861  
862  
863  
864  
865  
866  
867  
868  
869  
870  
871  
872  
873  
874  
875  
876  
877  
878  
879  
880  
881  
882  
883  
884  
885

286 The contaminated AT (epididymal left AT) were then grafted on uncontaminated host C57BL/6J  
287 mice. Figure 2 shows that TCDD concentration decreases in the TCDD-contaminated grafted tissue in  
288 a time dependent manner.



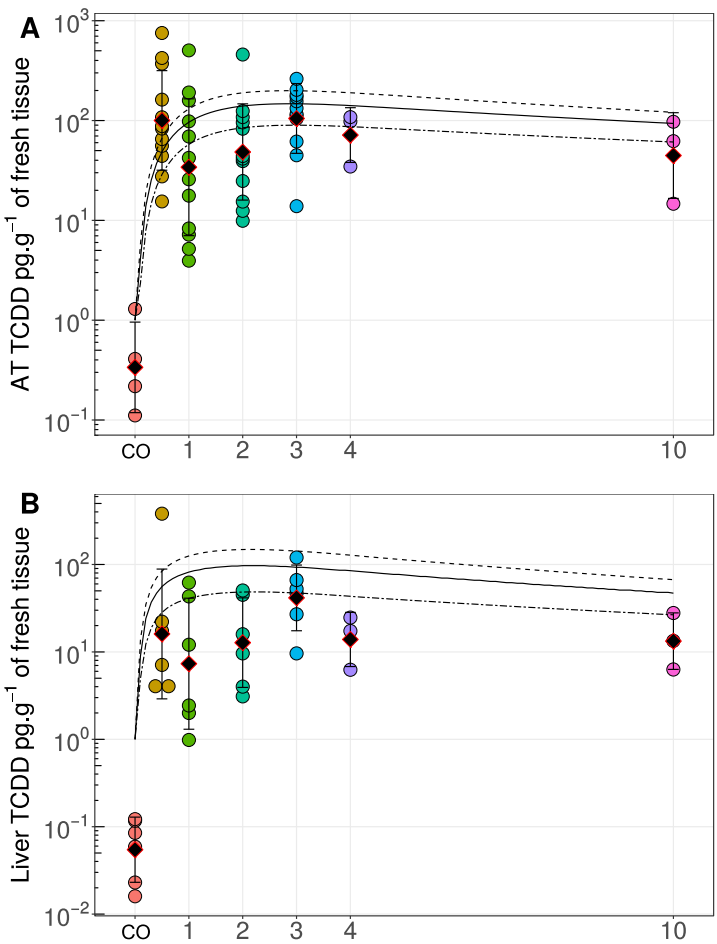
289  
290  
291  
**Figure 2:** Levels of TCDD (A: pg.g<sup>-1</sup> fresh tissue; B: pg.g<sup>-1</sup> lipid weight) measured in the grafted AT (3-6 mice/condition) at different time points following the graft (in weeks). The corn oil condition (CO) designates the level of TCDD present in a graft from mice injected with corn oil. In panel A, the line represents the profiled simulation of TCDD concentrations (expressed in pg TCDD.g<sup>-1</sup> fresh tissue) from the graft implanted in dorsal subcutaneous for 10 weeks.



886  
887  
888  
889  
890  
891  
892  
893  
894  
895  
896  
897  
898  
899  
900  
901  
902  
903  
904  
905  
906  
907  
908  
909  
910  
911  
912  
913  
914  
915  
916  
917  
918  
919  
920  
921  
922  
923  
924  
925  
926  
927  
928  
929  
930  
931  
932  
933  
934  
935  
936  
937  
938  
939  
940  
941  
942  
943  
944

292 **5.2 TCDD redistributes to other tissues**

293 Subsequently, we quantified the distribution of TCDD in three organs of the grafted mice,  
294 namely the epididymal AT of the host, liver and brain (respectively figures 3A and 3B, SFigure 2 Suppl.  
295 Mat). The levels of TCDD increased significantly in the host AT (figure 3A, from <1 to >100 pg.g<sup>-1</sup> of  
296 fresh tissue in 3 weeks) during the 3-week-time period and remained then stable over the course of  
297 the experiments. The distribution in the brain was slower than the distribution in the host AT, with a  
298 basal level of 0.1 pg.g<sup>-1</sup> of fresh tissue and a concentration that reached 1 pg.g<sup>-1</sup> of fresh tissue at 1  
299 week and 10 pg.g<sup>-1</sup> after 10 weeks (SFigure 2). The levels of TCDD also increased significantly in the  
300 liver (figure 3B, from <0.1 to >10 pg.g<sup>-1</sup> of fresh tissue in 2 weeks) during the 2-week-time period and  
301 remained then stable over the course of the experiments.



302 **Figure 3:** Levels of TCDD (pg.g<sup>-1</sup> of fresh tissue) in the host AT (A), and the liver (B) (n=6 mice/condition  
303 except weeks 4 and 10) at different time points following the graft (in weeks). For all panels, the  
304 symbols (●) represent the individual measurement and the symbols (◆) represents the mean  
305 measurement and the standard deviation of the TCDD measured (mean ± SD) at different time points  
306 following the sacrifice. (A) simulation curves of the TCDD accumulation and experimental values in the

AT and (B) in the liver issued from the host following subcutaneous grafting. For each of these tissues, we simulate the mean concentration at time 0, and the concentrations corresponding to the mean  $\pm$  SD (see text). The corn oil condition (CO) designates the level of TCDD present in a graft from mice injected with corn oil.

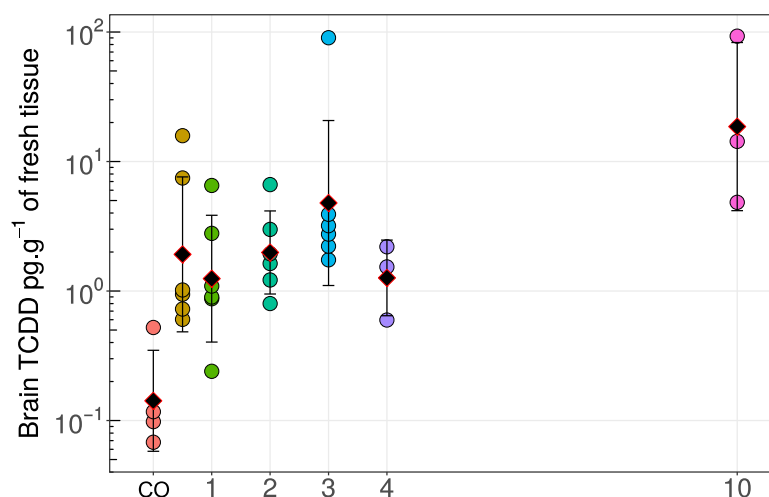


**Figure 2:** Levels of TCDD (pg.g<sup>-1</sup> of fresh tissue) in the brain (n=6 mice/condition except weeks 4 and 10) at different time points following the graft (in weeks). For all panels, the symbols (●) represent the individual measurement and the symbols (◆) represents the mean measurement and the standard deviation of the TCDD measured (mean  $\pm$  SD) at different time points following the sacrifice. The corn oil condition (CO) designates the level of TCDD from mice injected with corn oil.

When the levels of TCDD were represented in pg.g<sup>-1</sup> of lipid weight (SFigure 3, Suppl. Mat.), a similar profile was obtained for the AT, a tissue with a high fat content. The fast and slow accumulations of TCDD respectively in the liver and the brain were also clearly characterized.

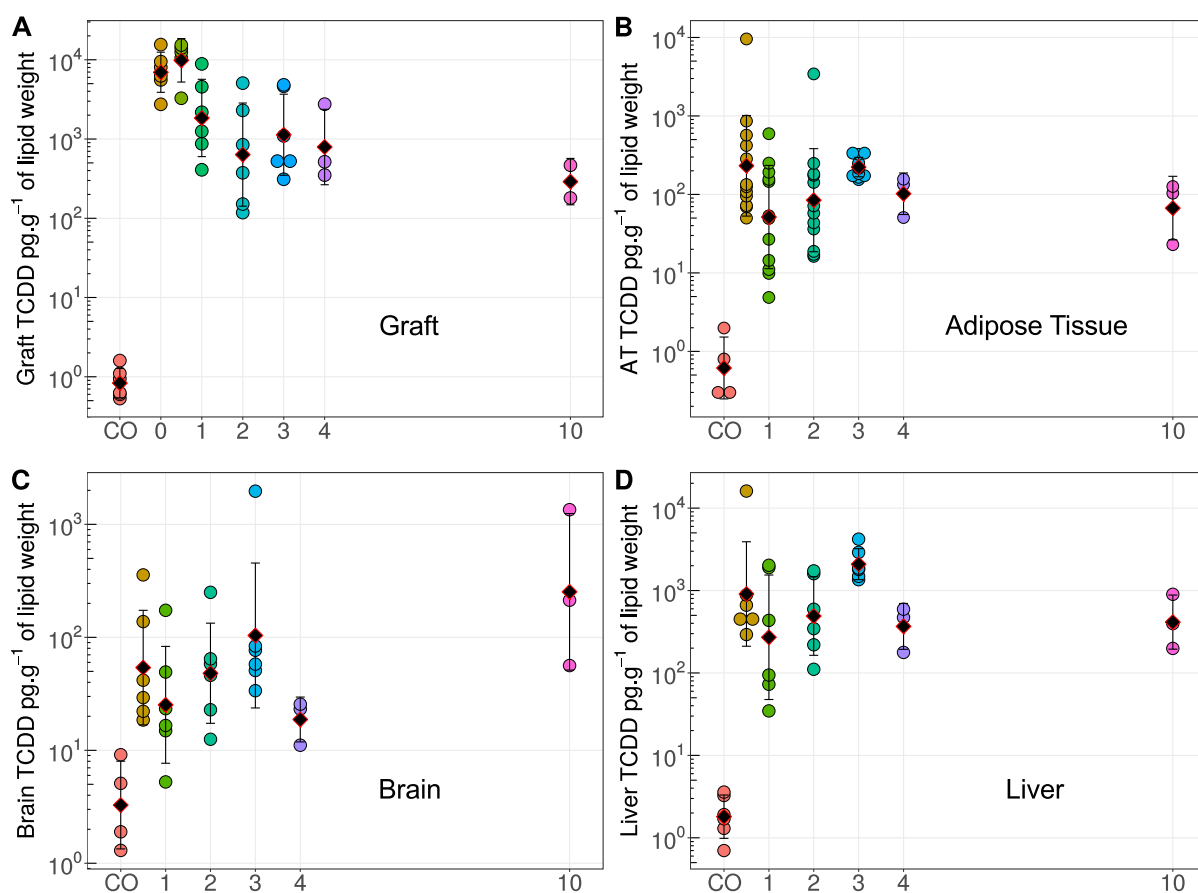


**Figure 3:** Levels of TCDD ( $\text{pg}\cdot\text{g}^{-1}$  lipid weight.) in the graft (A), host AT (B), brain (C) and liver (D) tissues ( $n=3-6$  mice/condition) at different time points following the graft ( $w$ : weeks). The corn oil condition (CO) designates the level of TCDD present in a graft from mice injected with corn oil.

Overall, our experiments demonstrate that TCDD is quickly released from a contaminated grafted-AT and redistributed in several key organs of the grafted C57BL6 mice albeit with different kinetics.

### 5.3 PBPK modeling - exposure of the donor

The first step consisted to simulate the exposure of donor mice to a single intraperitoneal injection dose at concentrations of 1, 10 and 25  $\mu\text{g}$  TCDD per kg bw (STable 2, Suppl. Mat.). Using the PBPK mouse model, we simulated the profile of TCDD concentrations in the AT (SFigure 4, Suppl. Mat.).

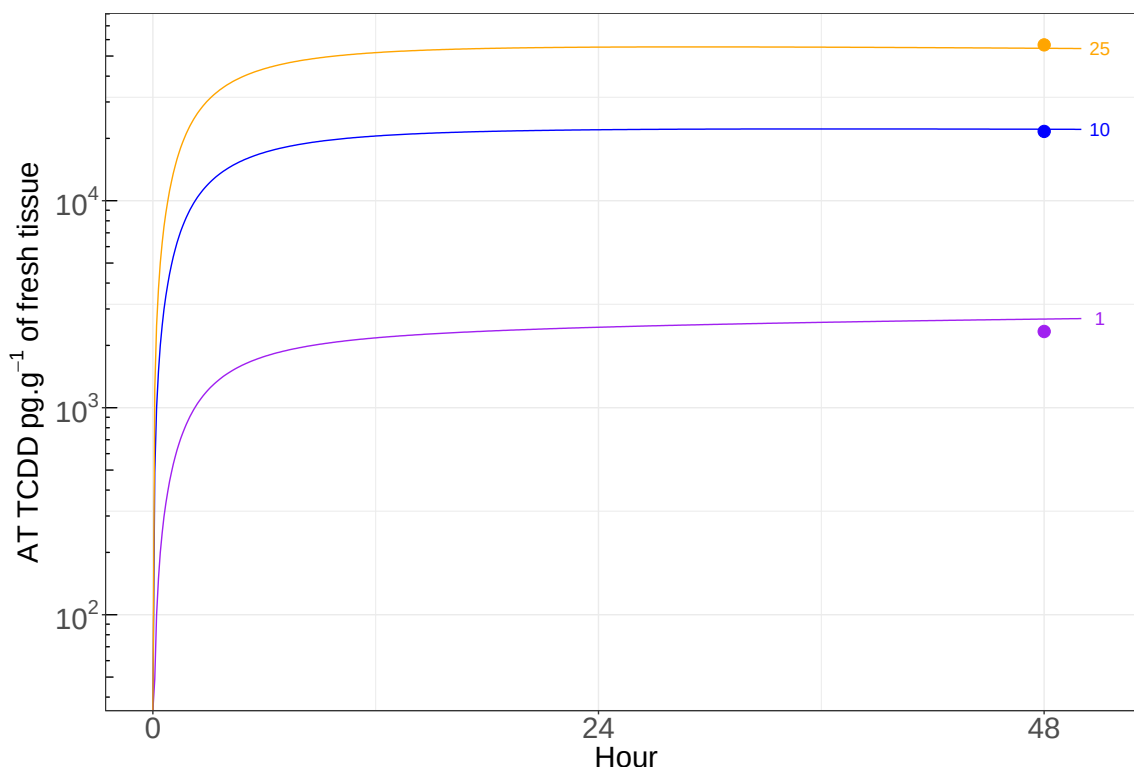


**Figure 4:** TCDD concentration in mouse AT following a single exposure of TCDD intraperitoneal at 1, 10 or 25 µg.kg<sup>-1</sup> body weight. The lines depict simulated concentrations and symbols the experimental data at 48h post exposure (see Supplementary table S2).

The simulation matched the experimental measurements of TCDD with very high accuracy (STable 2, Suppl. Mat. and SFigure 4, Suppl. Mat.) and the ratio of the nominal TCDD doses matched well with that of the measured TCDD concentrations in AT (Eq.4).

**Equation 4: Comparisons between ratio of dose and tissue concentrations:**

$$\frac{\frac{10\mu\text{g}}{\text{kg}}}{1\mu\text{g}/\text{kg}} \cong \frac{\frac{21623\text{pg}}{\text{gtissue}}}{\frac{2335\text{pg}}{\text{gtissue}}} \cong 10 \quad \frac{\frac{25\mu\text{g}}{\text{kg}}}{1\mu\text{g}/\text{kg}} \cong \frac{\frac{56608\text{pg}}{\text{gtissue}}}{\frac{2335\text{pg}}{\text{gtissue}}} \cong 25$$

#### 5.4 PBPK modeling - release of TCDD from the graft / distribution of TCDD in host compartments

The second step consisted of simulating the decrease of TCDD in the graft. Because of the large standard deviations, we used the mean of TCDD concentrations measured in the different assays (4815 pg.g<sup>-1</sup> fresh tissue at time 0). The first-order elimination rate constant was fixed at 0.004 h<sup>-1</sup>. The concentration of TCDD in the graft was about 85 pg.g<sup>-1</sup> fresh tissue at 10 weeks (corresponding to an elimination of 98.23%). The calculated half-life base based on the sequential point was 1.03 weeks on the first part of the biphasic curve (and 5.53 weeks for the second part of the curve).

1122  
1123  
1124 335 We also simulated the accumulation of TCDD concentrations in the host AT and liver  
1125  
1126 336 compartments following insertion of the graft. These compartments concentrate more than 90% of  
1127 337 the TCDD (Carrier, 1995). However, because the standard deviation (SD) of the initial concentration  
1128  
1129 338 reflecting the amount of TCDD in the graft was relatively large, the simulation was performed using 1)  
1130 339 the mean of the concentrations in the graft, 2) this mean + SD or 3) this mean - SD. Thus, for each  
1131  
1132 340 compartment, 2 curves were simulated (Figure 3). The prediction of the model was also accurate as  
1133 341 the experimental data points for the liver and the AT were found between each maximal and minimal  
1134  
1135 342 simulating curve (Figure 3).  
1136

1137 343 Overall, these two simulations (release and distribution) improved the confidence in the PBPK  
1138  
1139 344 model for mice.  
1140

### 1141 345 1142 1143 346 **5.5 TCDD release from AT alters the expression of metabolic genes** 1144

1145 347 We next investigated whether the TCDD released from graft-contaminated fat pad could alter  
1146 348 expression of genes coding for TCDD-target genes, *i.e.* key biologic or disease-related functions. We  
1147 349 and others have previously demonstrated that TCDD induced inflammation and fibrosis in the liver of  
1148  
1149 350 exposed mice (Duval et al., 2017). Thus, we studied several biomarkers that could be related to chronic  
1150 351 liver diseases (*i.e.* fibrosis, steatosis). We carried out RT-qPCR experiments using host liver and AT  
1151  
1152 352 samples at 3 weeks after grafting.  
1153  
1154

1155 353 We show that the levels of expression of AhR-target genes in the liver and AT were higher than  
1156 354 at time 0, a result in line with a rapid contamination of these organs (Tables 1 and 2). In addition, the  
1157 355 expression of fibrotic and inflammatory markers augmented also significantly, in line with our former  
1158  
1159 356 studies on TCDD treated mice (Duval et al., 2017). The host AT also displayed an inflammatory profile  
1160 357 (Table 2).  
1161  
1162  
1163  
1164  
1165  
1166  
1167  
1168  
1169  
1170  
1171  
1172  
1173  
1174  
1175  
1176  
1177  
1178  
1179  
1180

1181  
 1182  
 1183 358  
 1184  
 1185 359  
 1186  
 1187 360  
 1188  
 1189 361  
 1190  
 1191 362  
 1192  
 1193 363  
 1194  
 1195 364  
 1196  
 1197 365  
 1198  
 1199 366  
 1200  
 1201 367  
 1202  
 1203 368  
 1204  
 1205 369  
 1206  
 1207 370  
 1208  
 1209 371  
 1210  
 1211 372  
 1212  
 1213 373  
 1214  
 1215 374  
 1216  
 1217 375  
 1218  
 1219 376  
 1220  
 1221 377  
 1222  
 1223 378  
 1224  
 1225  
 1226  
 1227  
 1228  
 1229  
 1230  
 1231  
 1232  
 1233  
 1234  
 1235  
 1236  
 1237  
 1238  
 1239

Function	Genes	Fold ind.
XME	AhR	2.65
	CYP1A1	8.96**
	CYP1B1	3.62**
Inflammation	IL-1 $\beta$	4.17**
	IL-6	1.25
	TNF alpha	1.94
	MCP-1	5.98**
	NOS2	2.42
	F4/80	3.42**
Fibrosis	COL1A1	3.93**
	Alpha-SMA	4.51**
Metabolism	Glycogen synthase 2	3.17**
	PC	3.01**
	Cytosolic PEPCK	2.94**
	G6Pase	2.39**
	PGC-1 alpha	2.24**

**Table 1: Relative mRNA level of XME, inflammatory, fibrotic and metabolic marker in the liver following a 3-week internal exposure (statistically significant: \*\* p<0.01, 6 animals per condition).**

1240  
 1241  
 1242 379  
 1243  
 1244  
 1245  
 1246  
 1247  
 1248  
 1249  
 1250  
 1251  
 1252  
 1253  
 1254  
 1255  
 1256  
 1257  
 1258  
 1259  
 1260  
 1261  
 1262  
 1263  
 1264  
 1265  
 1266  
 1267  
 1268  
 1269  
 1270  
 1271  
 1272  
 1273  
 1274  
 1275  
 1276  
 1277  
 1278  
 1279  
 1280  
 1281  
 1282  
 1283  
 1284  
 1285  
 1286  
 1287  
 1288  
 1289 380  
 1290  
 1291 381  
 1292 382  
 1293 383  
 1294  
 1295  
 1296  
 1297  
 1298

Function	Genes	Fold ind.
XME	AhR	0.88
	CYP1A1	2.55*
	PAI-1	15.92*
	IL-6	9.4**
	IL10	2.4
Inflammation	TNF alpha	2.01*
	MCP-1	1.83*
	NOS2	1.35*
	CD68	2.79**
	ATGL	1.67*
	HSL	0.66
	CPT1B	1.34
Metabolism	VLCAD	2.10*
	AQP7	1.23
	CD36	0.49
	Cytosolic PECK	1.24*
	Glycerol Kinase	0.06*
	PK4	3.82*
	PGC-1 alpha	1.18
	FABP4	3.93
	PPAR $\alpha$	0.85
	FAS	1.74
	UCP1	1.99*
PPAR $\gamma$ 2	1.42	

**Table 2: Relative mRNA expression of several XME, inflammatory, fibrotic and metabolic markers in the AT following a 3-week internal exposure (statistically significant: \* p<0.05; \*\* p<0.01, 6 animals per condition).**

1299  
1300  
1301  
1302  
1303  
1304  
1305  
1306  
1307  
1308  
1309  
1310  
1311  
1312  
1313  
1314  
1315  
1316  
1317  
1318  
1319  
1320  
1321  
1322  
1323  
1324  
1325  
1326  
1327  
1328  
1329  
1330  
1331  
1332  
1333  
1334  
1335  
1336  
1337  
1338  
1339  
1340  
1341  
1342  
1343  
1344  
1345  
1346  
1347  
1348  
1349  
1350  
1351  
1352  
1353  
1354  
1355  
1356  
1357

384                    Due to the role of pyruvate carboxylase (PC), cytosolic phosphoenolpyruvate carboxykinase  
385 (PEPCK) and glucose 6 Phosphatase (G6Pase) in maintaining glycemia (potentially linked to type 2  
386 diabetes), we investigated the expression of their genes in the liver and found that their mRNA content  
387 increased from time 0 to time 3-weeks following grafting.

388  
389



1358  
1359  
1360  
1361  
1362  
1363  
1364  
1365  
1366  
1367  
1368  
1369  
1370  
1371  
1372  
1373  
1374  
1375  
1376  
1377  
1378  
1379  
1380  
1381  
1382  
1383  
1384  
1385  
1386  
1387  
1388  
1389  
1390  
1391  
1392  
1393  
1394  
1395  
1396  
1397  
1398  
1399  
1400  
1401  
1402  
1403  
1404  
1405  
1406  
1407  
1408  
1409  
1410  
1411  
1412  
1413  
1414  
1415  
1416

## 390 6. Discussion

391 In the present study we provide direct experimental evidence for the release of TCDD from  
392 adipose tissue (AT, graft) and its migration into other tissues. We also show that the released pollutant  
393 induces relevant changes in gene expression in the target tissues and we characterize the kinetics of  
394 its distribution. The study was designed to address a knowledge gap and a methodological gap. Indeed,  
395 one of the most challenging issues in environmental toxicity is to understand and model long-  
396 term/low-dose effects (Barouki, 2010). Concerning POPs, such long-term effects are usually explained  
397 by continuous exposure due to the persistence and bioaccumulation of those pollutants in the  
398 environment and by continuous release from internal storage sites such as the AT. It was not clear  
399 whether release from the AT was significant and whether it could induce biological or toxic effects in  
400 other tissues. Evidence for the latter mechanism has been gathered indirectly for example by studying  
401 weight loss in obese humans (Kim et al., 2011). The present study addresses specifically this point and  
402 provides direct evidence for the release of a POP from AT and describes its effects on other tissues.  
403 Thus, release of POPs from AT is likely to play a significant role in long-term effects of pollutants.

404 In order to study the release of POPs from the AT and its properties, we developed an adequate  
405 experimental model based on grafting of AT from a contaminated animal into a non-contaminated  
406 one. It explores the effects of a continuous release from an internal compartment, the AT and reflects  
407 exposures of humans and animals to POPs. Other models of continuous release do exist such as release  
408 capsules which have been designed mostly for pharmacological purposes (i.e. treatment of chronic  
409 pain) or micro-osmotic pumps (Mercadante, 2017; Tauer et al, 2013); however, both models differ  
410 from our model in the nature of the delivery compartment which is biologically relevant in our case  
411 and includes adipocytes, endothelial and immune cells which could influence the release. In that sense,  
412 the model described here is a better representation of the actual internal exposure than artificial  
413 models. However, it has its limitations too in that the graft could undergo different stresses and  
414 outcomes such a fibrosis or altered vascularization which may influence the observed results.

415 This AT graft model is clearly complementary to more traditional exposure models through  
416 ingestion or injection. It is not meant to be an alternative to other models but rather to identify the  
417 contributions of internal sources as compared to external exposures. In that sense it can help in  
418 assessing long-term effects even after withdrawal of external exposures. The model also allows the  
419 derivation of relevant toxicokinetic and toxicodynamic features that are complementary to those  
420 derived from classical drug treatment regimens.

421 Our experimental data improve the confidence in the PBPK model for mice that was developed  
422 previously (USEPA, 2012), and adapted for the present work. The intraperitoneal exposures to 1, 10

1417  
1418  
1419  
1420  
1421  
1422  
1423  
1424  
1425  
1426  
1427  
1428  
1429  
1430  
1431  
1432  
1433  
1434  
1435  
1436  
1437  
1438  
1439  
1440  
1441  
1442  
1443  
1444  
1445  
1446  
1447  
1448  
1449  
1450  
1451  
1452  
1453  
1454  
1455  
1456  
1457  
1458  
1459  
1460  
1461  
1462  
1463  
1464  
1465  
1466  
1467  
1468  
1469  
1470  
1471  
1472  
1473  
1474  
1475

423 and 25  $\mu\text{g.kg}^{-1}$  of body weight were also modeled (SFigure 4, Suppl. Mat.). The model accurately  
424 reproduces the experimental measurements, 48 hours following the single intraperitoneal  
425 administration for all doses, regarding the ratio of doses and the amount measured in tissues (Equation  
426 1). Yet, the model has its limitations since it requires surgery and some of the effects could be biased  
427 by the fate of the graft. Indeed, we observed individual differences in vascularization or fibrosis, which  
428 could impact TCDD release from the graft. These observations could partly explain why between 4 to  
429 10 weeks, the slope of TCDD elimination from the graft, changes (Figure 3); a better characterization  
430 of the vascularization of the graft will be necessary for our on-going projects. We believe that besides  
431 the structural variabilities described previously, metabolic adaptations and heterogenous lipid content  
432 could also influence TCDD release. A better characterization of the graft would improve the description  
433 of the PBPK model. However, at this point, it predicts with accuracy the evolution of TCDD  
434 concentrations in both AT and liver known as the most important depository organs of this pollutant  
435 in mammals. Indeed, our experimental data that match the PBPK model, indicate that despite some  
436 variability in the initial concentrations of TCDD in the graft (mean of  $4815 \pm 2122 \mu\text{g.kg}^{-1}$ ), the POP  
437 diffuses to other key organs such as the host AT, liver or brain following different kinetics. The release  
438 of TCDD from the graft is relatively rapid with a half-life of 1.03 weeks ( $\cong 173$  hours, from weeks 0-4)  
439 and 5.53 weeks (932 hours from week 4), suggesting that after 10 weeks, more than 97% has been  
440 released from the graft. The modeled kinetics of release and distribution is in line with the  
441 experimental data (Figure 3); this simulation represents an exciting predictive tool which also could be  
442 improved in the future using a wider range of POPs and representative mixtures.

443  
444 The release of TCDD influences important biological pathways that are involved in liver and AT  
445 dysfunction. For this part of the work, the focus was first on xenobiotic metabolizing enzymes  
446 (biomarkers of an activated AhR signaling pathway) and inflammatory cytokines/chemokines which  
447 are classically induced upon TCDD exposure. As expected (regarding the distribution of TCDD), the AhR-  
448 target genes (CYP1A1, CYP1B1, PAI-1) were significantly induced at the mRNA levels in the liver and AT  
449 3 weeks following grafting (Tables 1 and 2). Similarly, an inflammatory signature is observed in both  
450 tissues which is in line with the literature and our former studies using traditional modes of exposure  
451 (Duval *et al.* 2017; Kim *et al.* 2011, 2012). Furthermore, a highly significant increase of the expression  
452 of two biomarkers of fibrosis in the liver (alpha-Smooth Muscle Action or alpha-SMA and collagen 1A1  
453 or COL1A1IL) was obtained, confirming our recent observations on the occurrence of liver fibrosis  
454 following exposure to TCDD (Duval *et al.* 2017). Finally, the mRNA expression of the three key  
455 gluconeogenic enzymes, pyruvate carboxylase (PC), cytosolic phosphoenolpyruvate carboxykinase  
456 (PEPCK), glucose 6-phosphatase (G6Pase) showed significant inductions. Such enzymes contribute to  
457 the maintenance of glycemia during fasting, but their induction is also classically described in type 2

1476  
1477  
1478  
1479  
1480  
1481  
1482  
1483  
1484  
1485  
1486  
1487  
1488  
1489  
1490  
1491  
1492  
1493  
1494  
1495  
1496  
1497  
1498  
1499  
1500  
1501  
1502  
1503  
1504  
1505  
1506  
1507  
1508  
1509  
1510  
1511  
1512  
1513  
1514  
1515  
1516  
1517  
1518  
1519  
1520  
1521  
1522  
1523  
1524  
1525  
1526  
1527  
1528  
1529  
1530  
1531  
1532  
1533  
1534

457 diabetes (Beale *et al.*, 2007). These results are different from those of other teams who reported that  
458 expression of PEPCK is strongly repressed by TCDD; in 1993, Stahl *and coll.* demonstrated that TCDD  
459 exposure decreased hepatic gluconeogenesis due to a reduction of PEPCK activity and mRNA  
460 expression (Stahl *et al.*, 1993) which has been also observed in another model by Dunlap *and coll*  
461 (Dunlap *et al.*, 2002). This was also demonstrated for PC following a short treatment in hepatic rat  
462 livers (Ilian *et al.*, 1996). We hypothesize that the difference between those observations and our data  
463 is due to the mode of exposure; most previous experiments were performed using an acute-based  
464 exposure protocol while our model allows a constant delivery of TCDD for several weeks. While we are  
465 not able at this point to explain mechanistically the differences, we think that a sustained low-dose  
466 delivery of TCDD could have a different impact than an acute delivery of TCDD, on the regulation of  
467 gluconeogenesis enzymes.

468 This observation suggests that a continuous exposure of TCDD could disrupt carbohydrate and  
469 lipid metabolism and, more generally, liver functions. Thus, the TCDD released from an internal storage  
470 site can induce gene expression changes in at least two tissues that reflect biological activity of this  
471 pollutant and which is in line with what is known about its toxicity. While it is likely that some of the  
472 effects of TCDD on gene expression are related to the activation of the AhR pathway (such as the  
473 induction of CYP1 genes), other effects may be indirect. For example, TCDD and the AhR activate the  
474 expression of inflammatory cytokines through direct or indirect, genomic or non-genomic pathways  
475 (Kim *et al.* 2012), and those cytokines could also be responsible for the other genomic alterations  
476 observed in the liver and the AT; moreover, as the release of TCDD from the graft is relatively rapid  
477 and then high, these gene expressions could represent an adaptive response to a major environmental  
478 stress (a high dose of TCDD). In order to delineate the actual mechanisms involved in the effects of  
479 contaminated/xenografted-AT on gene expression in distant tissues after such periods of exposure (3  
480 weeks in our case), additional studies would be required. Thus, we can conclude that the release of  
481 POPs from internal storage sites could play a significant role in the toxicity of those pollutants that  
482 needs to be further investigated using a wider range of POPs and representative mixtures.

483  
484 **7. Conclusion**

485 The experimental model described here represents a novel approach to explore exposure to  
486 pollutants from endogenous sources and their long-term toxicities. It is meant to be complementary  
487 to other experimental protocols of exposure through diet, dermal, intraperitoneal injection or gavage  
488 procedures.

1535  
1536  
1537  
1538  
1539  
1540  
1541  
1542  
1543  
1544  
1545  
1546  
1547  
1548  
1549  
1550  
1551  
1552  
1553  
1554  
1555  
1556  
1557  
1558  
1559  
1560  
1561  
1562  
1563  
1564  
1565  
1566  
1567  
1568  
1569  
1570  
1571  
1572  
1573  
1574  
1575  
1576  
1577  
1578  
1579  
1580  
1581  
1582  
1583  
1584  
1585  
1586  
1587  
1588  
1589  
1590  
1591  
1592  
1593

## 490 8. References

- 491 Ambolet-Camoit, A., Ottolenghi, C., Leblanc, A., Kim, M-J., Letourneur, F., Jacques, S., Cagnard, N.,  
492 Guguen-Guillouzo, C., Barouki, R., Aggerbeck, M., 2015. Two persistent organic pollutants  
493 which act through different xenosensors (alpha-endosulfan and 2,3,7,8 tetrachlorodibenzo-p-  
494 dioxin) interact in a mixture and downregulate multiple genes involved in human hepatocyte  
495 lipid and glucose metabolism. *Biochimie* 116, 79-91.
- 496 Barouki, R., 2010. Linking long-term toxicity of xeno-chemicals with short-term biological adaptation.  
497 *Biochimie* 92, 1222-1226. <https://doi.org/10.1016/j.biochi.2010.02.026>
- 498 Beale, E.G., Harvey, B.J., Forest, C., 2007. PCK1 and PCK2 as candidate diabetes and obesity genes. *Cell*  
499 *Biochem. Biophys.* 48, 89-95.
- 500 Birnbaum, L.S., 1995. Developmental effects of dioxins. *Environ. Health Perspect.* 103 Suppl 7, 89-94.
- 501 Boffetta, P., Mundt, K.A., Adami, H-O., Cole, P., Mandel, J.S., 2011. TCDD and cancer: a critical review  
502 of epidemiologic studies. *Crit. Rev. Toxicol.* 41, 7, 622-636.
- 503 Bonde, J.S., Flachs, E.M., Rimborg, S., Glazer, C.H., Giwercman, A., 2016. The epidemiologic evidence  
504 linking prenatal and postnatal exposure to endocrine disrupting chemicals with male  
505 reproductive disorders: a systematic review and meta-analysis. *Hum. Reprod. Update.* 23, 104-  
506 125.
- 507 Brown, R.P., Delp, M.D., Lindstedt, S.L., Rhomberg, L.R., Beliles, R.P., 1997. Physiological Parameter  
508 Values for Physiologically Based Pharmacokinetic Models. *Toxicol. Ind. Health* 13, 407-484.  
509 <https://doi.org/10.1177/074823379701300401>
- 510 Carrier, G., 1995. Modeling of the Toxicokinetics of Polychlorinated Dibenzo-p-dioxins and  
511 Dibenzofurans in Mammals, Including Humans I. Nonlinear Distribution of PCDD/PCDF Body  
512 Burden between Liver and Adipose Tissues. *Toxicol. Appl. Pharmacol.* 131, 253-266.  
513 <https://doi.org/10.1006/taap.1995.1068>
- 514 Chevrier, J., Dewailly, E., Ayotte, P., Mauriège, P., Després, J.P., Tremblay, A., 2000. Body weight loss  
515 increases plasma and adipose tissue concentrations of potentially toxic pollutants in obese  
516 individuals. *Int J Obes Relat Metab Disord.* 24, 10, 1272-8.
- 517 Costera, A., Feidt, C., Marchand, P., Le Bizec, B., Rychen, G., 2006. PCDD/F and PCB transfer to milk in  
518 goats exposed to a long-term intake of contaminated hay. *Chemosphere.* 64, 4, 650-657.
- 519 Diliberto, J.J., Burgin, D., Birnbaum, L.S., 1997. Role of CYP1A2 in hepatic sequestration of dioxin:

1594  
1595  
1596 520 studies using CYP1A2 knock-out mice. *Biochem. Biophys. Res. Commun.* 236, 431–433.  
1597  
1598 521 <https://doi.org/10.1006/bbrc.1997.6973>  
1599  
1600 522 Dunlap, D.Y., Ikeda, I., Nagashima, H., Vogel, C.F., Matsumura, F, 2002. Effects of src-deficiency on the  
1601  
1602 523 expression of in vivo toxicity of TCDD in a strain of c-src knockout mice procured through six  
1603 524 generations of backcrossings to C57BL/6 mice. *Toxicology.* 172, 125-41.  
1604  
1605 525 Duval, C., Teixeira-Clerc, F., Leblanc, A.F., Touch, S., Emond, C., Guerre-Millo, M., Lotersztajn, S.,  
1606 526 Barouki, R., Aggerbeck, M., Coumoul, X., 2017. Chronic Exposure to Low Doses of Dioxin  
1608 527 Promotes Liver Fibrosis Development in the C57BL/6J Diet-Induced Obesity Mouse Model.  
1609  
1610 528 *Environ Health Perspect.* 125, 428-436.  
1611  
1612 529 Emond, C., 2004. Physiologically Based Pharmacokinetic Model for Developmental Exposures to TCDD  
1613  
1614 530 in the Rat. *Toxicol. Sci.* 80, 115–133. <https://doi.org/10.1093/toxsci/kfh117>  
1615  
1616 531 Emond, C., Birnbaum, L.S., DeVito, M.J., 2006. Use of a physiologically based pharmacokinetic model  
1617 532 for rats to study the influence of body fat mass and induction of CYP1A2 on the  
1618  
1619 533 pharmacokinetics of TCDD. *Environ. Health Perspect.* 114, 1394–1400.  
1620  
1621 534 Emond, C., DeVito, M.J., Diliberto, J.J., Birnbaum, L.S., 2018. The Influence of Obesity on the  
1622  
1623 535 Pharmacokinetics of Dioxin in Mice: An Assessment Using Classical and PBPK Modeling.  
1624 536 *Toxicol. Sci.* <https://doi.org/10.1093/toxsci/kfy078>  
1625  
1626 537 Emond, C., Michalek, J.E., Birnbaum, L.S., DeVito, M.J., 2005. Comparison of the use of a physiologically  
1627  
1628 538 based pharmacokinetic model and a classical pharmacokinetic model for dioxin exposure  
1629  
1630 539 assessments. *Environ. Health Perspect.* 113, 1666–1668.  
1631  
1632 540 Emond, C., Ruiz, P., Mumtaz, M., 2017. Physiologically based pharmacokinetic toolkit to evaluate  
1633 541 environmental exposures: Applications of the dioxin model to study real life exposures.  
1634  
1635 542 *Toxicol. Appl. Pharmacol.* 315, 70–79. <https://doi.org/10.1016/j.taap.2016.12.007>  
1636  
1637 543 Emond, C., DeVito, M., Warner, M., Eskenazi, B., Mocarelli, P., Birnbaum, L.S., 2016. An assessment of  
1638 544 dioxin exposure across gestation and lactation using a PBPK model and new data from Seveso.  
1639  
1640 545 *Environ Int.* 92-93, 23-32.  
1641  
1642 546 Emond, C., Raymer, J.H., Studabaker, W.B., Garner, C.E., Birnbaum, L.S., 2010. A physiologically based  
1643 547 pharmacokinetic model for developmental exposure to BDE-47 in rats. *Toxicol Appl*  
1644  
1645 548 *Pharmacol.* 242, 290-8.  
1646  
1647 549 Gasiewicz, T.A., Geiger, L.E., Rucci, G., Neal, R.A., 1983. Distribution, excretion, and metabolism of  
1648  
1649 550 2,3,7,8-tetrachlorodibenzo-p-dioxin in C57BL/6J, DBA/2J, and B6D2F1/J mice. *Drug Metab.*  
1650  
1651  
1652

1653  
1654  
1655 551 Dispos. Biol. Fate Chem. 11, 397–403.  
1656  
1657 552 Goodman, M., Narayan, K.M.V., Flanders, D., Chang, E.T., Adami, H-O., Boffetta, P., Mandel, J.S., 2015.  
1658  
1659 553 Dose-Response Relationship Between Serum 2,3,7,8-Tetrachlorodibenzo-p-Dioxin and  
1660  
1661 554 Diabetes Mellitus: A Meta-Analysis. American Journal of Epidemiology. 181, 6, 374.  
1662  
1663 555 Guyot, E., Chevallier, A., Barouki, R., Coumoul, X., 2013. The AhR twist: ligand-dependent AhR signaling  
1664 556 and pharmaco-toxicological implications. Drug Discov. Today. 18, 479-486.  
1665  
1666 557 Ilian, M.A., Sparrow, B.R., Ryu, B.W., Selivonchick, D.P., Schaup, H.W., 1996. Expression of  
1667  
1668 558 hepatic pyruvate carboxylase mRNA in C57BL/6J Ah(b/b) and congenic Ah((d/d)) mice exposed  
1669  
1670 559 to 2,3,7,8-tetrachlorodibenzo-p-dioxin. J Biochem Toxicol. 11, 51-6.  
1671  
1672 560 Imbeault, P., Chevrier, J., Dewailly, E., Ayotte, P., Després, J.P., Mauriège, P., Tremblay, A, 2002.  
1673 561 Increase in plasma pollutant levels in response to weight loss is associated with the reduction  
1674  
1675 562 of fasting insulin levels in men but not in women. Metabolism. 51, 4, 482-6.  
1676  
1677 563 Juricek, L., Bui, L.-C., Busi, F., Pierre, S., Guyot, E., Lamouri, A., Dupret, J.-M., Barouki, R., Coumoul, X.,  
1678  
1679 564 Rodrigues-Lima, F., 2014. Activation of the aryl hydrocarbon receptor by carcinogenic aromatic  
1680 565 amines and modulatory effects of their N-acetylated metabolites. Arch. Toxicol.  
1681  
1682 566 <https://doi.org/10.1007/s00204-014-1367-7>  
1683  
1684 567 Kim, M.-J., Marchand, P., Henegar, C., Antignac, J.-P., Alili, R., Poitou, C., Bouillot, J.-L., Basdevant, A.,  
1685 568 Le Bizec, B., Barouki, R., Clément, K., 2011. Fate and complex pathogenic effects of dioxins and  
1686  
1687 569 polychlorinated biphenyls in obese subjects before and after drastic weight loss. Environ.  
1688  
1689 570 Health Perspect. 119, 377–383. <https://doi.org/10.1289/ehp.1002848>  
1690  
1691 571 Kim, M.-J., Pelloux, V., Guyot, E., Tordjman, J., Bui, L.-C., Chevallier, A., Forest, C., Benelli, C., Clément,  
1692 572 K., Barouki, R., 2012. Inflammatory pathway genes belong to major targets of persistent  
1693  
1694 573 organic pollutants in adipose cells. Environ. Health Perspect. 120, 508-514.  
1695  
1696 574 Kissel, J.C., Robarge, G.M., 1998. Assessing the elimination of 2,3,7,8-TCDD from humans with a  
1697 575 physiologically based pharmacokinetic model. Chemosphere 17, 2017–2027.  
1698  
1699 576 [https://doi.org/10.1016/0045-6535\(88\)90012-4](https://doi.org/10.1016/0045-6535(88)90012-4)  
1700  
1701 577 La Merrill, M., Emond, C., Kim, M.-J., Antignac, J.-P., Le Bizec, B., Clement, K., Birnbaum, L.S., Barouki, R  
1702  
1703 578 2013. Toxicological function of adipose tissue: focus on persistent organic pollutants. Environ.  
1704 579 Health Perspect. 121, 162-169.  
1705  
1706 580 Lee, Y.M., Kim, K.S., Jacobs, D.R., Lee, D.H., 2017. Persistent organic pollutants in adipose tissue should  
1707  
1708 581 be considered in obesity research. Obes Rev 18, 2, 129-139.  
1709  
1710  
1711

1712  
1713  
1714 582 Leung, H., Ku, R.H., Paustenbach, D.J., Andersen, M.E., 1988. A physiologically based pharmacokinetic  
1715  
1716 583 model for 2,3,7,8-tetrachlorodibenzo-p-dioxin in C57BL/6J and DBA/2J mice. *Toxicol Lett* 42,  
1717 584 15-28.  
1718  
1719 585 Leung, H., Paustenbach, D.J., Murray, F., Andersen, M.E., 1990. A physiological pharmacokinetic  
1720 586 description of the tissue distribution and enzyme-inducing properties of 2,3,7,8-  
1721 587 tetrachlorodibenzo-p-dioxin in the rat. *Toxicol Appl Pharmacol* 103, 399-410.  
1722  
1723  
1724 588 Mercadante, S., 2017. Oxycodone extended release capsules for the treatment of chronic pain. *Expert*  
1725 589 *Rev Neurother.* 17, 427-431  
1726  
1727  
1728 590 Mostafalou, S., 2016. Persistent Organic Pollutants and Concern Over the Link with Insulin Resistance  
1729 591 Related Metabolic Diseases. *Rev Environ Contam Toxicol* 238, 69-89.  
1730  
1731  
1732 592 Novelli, M., Piaggi, S., De Tata, V., 2005. 2,3,7,8-Tetrachlorodibenzo-p-dioxin-induced impairment of  
1733 593 glucose-stimulated insulin secretion in isolated rat pancreatic islets. *Toxicol. Lett.* 156, 2, 307-  
1734 594 314.  
1735  
1736  
1737 595 Pfaffl, M.W., 2001. A new mathematical model for relative quantification in real-time RT-PCR. *Nucleic*  
1738 596 *Acids Res.* 29, e45.  
1739  
1740  
1741 597 Smarr, M.M., Kannan, K., Buck Louis, G.M., 2016. Endocrine disrupting chemicals and endometriosis.  
1742 598 *Fertility and Sterility* 106, 4, 959-966.  
1743  
1744  
1745 599 Stahl, B.U., Beer, D.G., Weber, L.W., Rozman, K., 1993. Reduction of hepatic phosphoenolpyruvate  
1746 600 carboxykinase (PEPCK) activity by 2,3,7,8-tetrachlorodibenzo-p-dioxin (TCDD) is due to  
1747 601 decreased mRNA levels. *Toxicology.* 79, 81-95.  
1748  
1749  
1750 602 Tauer, J.T., Hofbauer, L.C., Jung, R., Erben, R.G., Suttorp, M., 2013. Micro-osmotic pumps for  
1751 603 continuous release of the tyrosine kinase inhibitor bosutinib in juvenile rats and its impact on  
1752 604 bone growth. *Med Sci Monit Basic Res.* 19, 274-8.  
1753  
1754  
1755 605 USEPA, 2012. EPA's reanalysis of key issues related to dioxin toxicity and response to NAS comments,  
1756 606 in: (EPA/600/R-10/038F), (EPA/600/R-10/038F).  
1757  
1758  
1759 607 Wang, X., Santostefano, M.J., Evans, M.V., Richardson, V.M., Diliberto, J.J., Birnbaum, L.S., 1997.  
1760 608 Determination of Parameters Responsible for Pharmacokinetic Behavior of TCDD in Female  
1761 609 Sprague-Dawley Rats. *Toxicol. Appl. Pharmacol.* 147, 151-168.  
1762  
1763 610 <https://doi.org/10.1006/taap.1997.8242>  
1764  
1765  
1766 611 White, S.S., Birnbaum, L.S., 2009. An overview of the effects of dioxins and dioxin-like compounds on  
1767  
1768  
1769  
1770

1771  
1772  
1773 612 vertebrates, as documented in human and ecological epidemiology. *J. Environ. Sci. Health Part*  
1774 *C Environ. Carcinog. Ecotoxicol. Rev.* 27, 197-211.  
1775 613  
1776 614 <https://doi.org/10.1080/10590500903310047>  
1777  
1778 615 Wolfe, W.H., Michalek, J.E., Miner, J.C., Pirkle, J.L., Caudill, S.P., Patterson, D.G., Needham, L.L., 1994.  
1779  
1780 616 Determinants of TCDD half-life in veterans of operation ranch hand. *J. Toxicol. Environ. Health*  
1781  
1782 617 41, 481-488. <https://doi.org/10.1080/15287399409531858>  
1783  
1784 618  
1785  
1786 619  
1787  
1788 620  
1789  
1790  
1791  
1792  
1793  
1794  
1795  
1796  
1797  
1798  
1799  
1800  
1801  
1802  
1803  
1804  
1805  
1806  
1807  
1808  
1809  
1810  
1811  
1812  
1813  
1814  
1815  
1816  
1817  
1818  
1819  
1820  
1821  
1822  
1823  
1824  
1825  
1826  
1827  
1828  
1829